Investigation of mechanical, microstructure, and corrosion properties of duplex stainless steel joint for natural gas processing facilities

by Sutrisna -

PAPER • OPEN ACCESS

Investigation of mechanical, microstructure, and corrosion properties of duplex stainless steel joint for natural gas processing facilities

IOP Conf. Series: Earth and Environmental Science 1151 (2023) 012056 doi:10.1088/1755-1315/1151/1/012056

Investigation of mechanical, microstructure, and corrosion properties of duplex stainless steel joint for natural gas processing facilities

D S Pamuji[1,*], M L Hakim[2], Sutrisna[1] and Novianto[3]

[1]Department of Mechanical Engineering, Faculty of Industrial Technology, Institut Teknologi Nasional Yogyakarta, Indonesia
[2]Department of Electrical Engineering Education, Universitas Negeri Yogyakarta, Indonesia
[3]Detech Material Testing Laboratory, Indonesia

*didit@itny.ac.id

Abstract. Duplex stainless steel is an exotic material known for its excellent corrosion resistance and mechanical properties due to the presence of a two-phase structure that is quite balanced between ferrite and austenite, making it one of the top choices for the oil and gas industry. In this paper, we will discuss the process and investigation of the welding results of the A/SA 790 UNS 31803 duplex pipe joint which is connected using the gas tungsten arc welding (GTAW) process for gas purification process applications. The welding process and qualification is based on the ASME BPVC Sec code. IX was then tested to obtain information on the characteristics of the mechanical properties, microstructure, and corrosion resistance of the resulting joints. Heat input in the welding process is a crucial factor that determines the equilibrium of the ferrite and austenite phases which then correlates with the mechanical properties and corrosion resistance of the joint. Based on the microstructural analysis, there was a decrease in the ferrite phase in the weld metal, but it was still within the required limits. Furthermore, the results of the mechanical properties test showed that the tensile strength of the joint was greater than the tensile strength of the base metal and no open discontinuity was observed in the bending test. The corrosion test showed no signs of pitting corrosion with a weight loss value of 1.7 g/m^2.

1. Introduction

Natural gas is a plentiful worldwide resource that burns cleanly and has significant environmental advantages when compared to other fossil fuels. Indonesia has the world's fourteenth largest proven natural gas reserves and the third largest in Asia-Pacific, accounting for an estimated 1.6% of total proven gas reserves. In 2013, Indonesia had 99.77 TCF of proved reserves and 50.21 TCF of prospective reserves, according to statistics from the Special Task Force for Upstream Oil and Gas Business Activities. The gas reserves in Indonesia are depicted in Figure 1. The majority of gas deposits are located offshore from Natuna, South Sumatra, East Kalimantan, Masela, and West Papua. The Natuna D-Aplha gas field is the largest in Southeast Asia (ASEAN), with an estimated 46 trillion cubic feet (TCF) of recoverable reserves with a high carbon dioxide component (71%), the majority of which is unexplored [1].

IOP Conf. Series: Earth and Environmental Science 1151 (2023) 012056 doi:10.1088/1755-1315/1151/1/012056

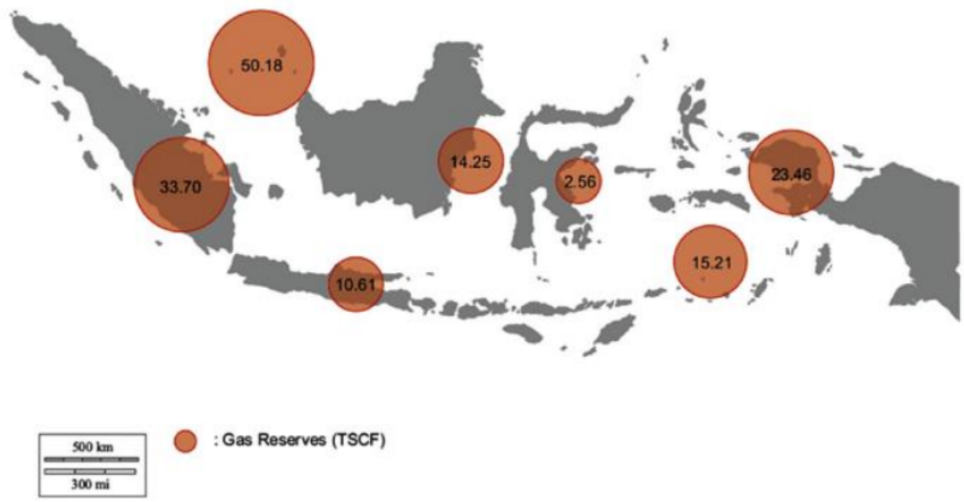

Figure 1. The gas reserve of Indonesia, adopted from [1]

However, natural gas contains water vapor and any pollutants when it exits the reservoir. Raw natural gas from production wells may contain carbon dioxide, hydrocarbons, water, hydrogen sulfide, nitrogen, and other contaminants [2]. Because most consumers have little need for raw gas, it may require several stages of processing before it can be purchased and used. The goal of a natural gas processing plant is to produce treated gas by reducing heavy hydrocarbons, acid gases, water, nitrogen, and other pollutants to acceptable levels that meet pipeline design and client requirements. Natural gas that does not meet specifications may create considerable issues due to pipeline corrosion and/or clogging, resulting in dangerous operation.

The composition of the input gas and the levels of processing required to meet product specifications and emission limits determine the structure and complexity of a gas processing plant. The amount of recovered NGL components can also be influenced by the liquid product values, which can make the process more complex. Figure 2 displays two streamlined concepts for gas processing plants. The first plan entails removing condensate, sulphur, and heavier components in order to meet sales gas specifications. The second tactic is to process the input gas for the recovery of each individual NGL component to increase plant profits.

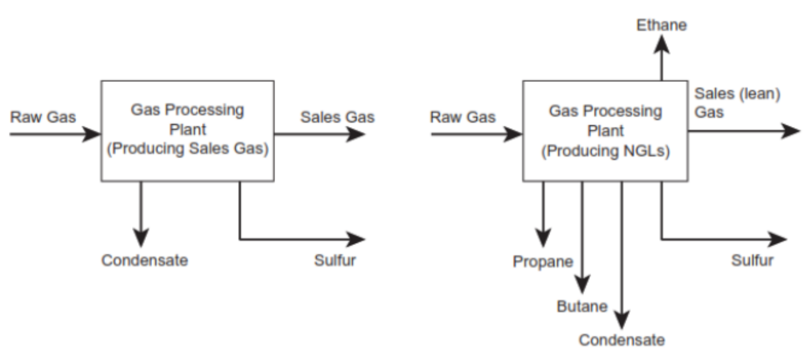

Figure 2. Two distinct natural gas processing plant schemes, adopted from [2]

Environmental conditions in the oil and gas exploration and processing fields require the use of materials having high corrosion resistance and strength. The use of 300 series stainless steel in harsh environment of oil and gas facilities has been abandoned and replaced by duplex stainless steel (DSS), which is composed of 50% austenite (γ) and 50% ferrite (α) phases in its microstructure. The advantages of each phase of austenite and ferrite combined into DSS, making it a very strong, tough, ductile and more corrosion resistant than austentic stainless steel [2]. Since roughly 35 years, duplex steels material have been employed in the oil and gas sector. It began with the usage of ASTM/ASME 1.4462/UNS S32205 (ASTM A240, ASTM A789/A790, ASTM A928). Another standard DSS used in oil and gas facilities is UNS S31803, which has slight difference in Mo composition than UNS32205. Meanwhile, Lean Duplex, Super Duplex, and Hyper Duplex grades are used based on the corrosion resistance and tensile strength requirements. In addition to the previously mentioned benefits of using Duplex steels, the oil and gas sector can benefit from two more major characteristics: First, exceptional resistance to corrosive media such as carbon dioxide, hydrogen sulphide, chlorides, and low ph-value media in compared to austenitic grades. Second, exceptional response to stress corrosion cracking (SCC) in high chloride environments in contrast to austenitic grades [3].

DSS has a wide range of application potential in oil and gas transportation because it addresses the performance issues with regular pipe and satisfies the complex oil and gas extraction and transportation environment requirements. However, welding on DSS is difficult due to problems like an unqualified A/F phase ratio and a weld joint with low corrosion resistance. Therefore, optimizing its welding performance in real-world engineering applications is essential. Although the austenite/ferrite ratio of the duplex stainless steels used in the oil and gas industry is roughly 50/50, the phase balance of duplex steels generally ranges from 35% to 65% ferrite [4]. The breakdown of the ferrite and precipitation of alpha prime occur at temperatures over 320°C (608°F) and up to about 550°C (1022°F) over an extended period of time. Duplex stainless steels are typically not used over 300°C (572°F) due to the severe loss of ductility caused by this phase [2].

Shielded metal arc welding (SMAW) [5], [6], submerged arc welding (SAW) [7], gas tungsten arc welding (GTAW) [5], [8], laser beam welding (LBW) [9], [10], plasma arc welding (PAW) [11], flux-cored arc welding (FCAW) [12], electron beam welding (EBW) [13], and friction assisted welding [14] are just a few of the processes that have been used to weld DSS by numerous researchers and engineers. However, a common processing technique that is frequently used in the production of DSS for engineering applications is fusion welding [15].

During the fusion welding process, the heat input greatly influences the phase formation in the microstructure. Especially if the welding is carried out in several layers, the interpass temperature must be considered to avoid shrinkage of the ferrite phase to alpha prime (α') at a temperature of around 475°C so that the material becomes brittle [4]. The greater the heat input experienced at the junction, the greater the probability of phase loss of the ferrite [16]. However, previous studies mostly discussed the DSS UNS 32205 material and very few reviewed the DSS UNS 31803 welded joint. Therefore, this paper aims to investigate the mechanical properties, microstructure, and corrosion resistance of the DSS UNS 31803 welded joint used in natural gas facilities.

2. Material and Method

The test material is DSS UNS 31803 pipe with an outer diameter (OD) of 169.51 mm and a wall thickness of 11.27 mm, also known as pipe 6 inch sch.80, welded using full manual GTAW with electrode ER2209. The base metal grouping based on ASME Boiler and Pressure Vessel Code Sec. IX 2019, in QW/QB-422 are shown in Table 1 [17]. The chemical composition of the base metal and electrode used are shown in Table 2 and Table 3, respectively. The groove shape and welding sequence consist of root pass, hot pass, fill pass, and capping are shown in Figure 3. The welding parameter for manual GTAW with up hill direction and 6G position are shown in Table 4. In the welding process, the interpass temperature is measured and maintained not to exceed 150°C.

Following the welding test, the microstructure was examined using an optical microscope (OM) to count the amount of ferrite using the ASTM E562 standard, followed by a pitting corrosion test using

ASTM G-48 method A, and mechanical testing as required by ASME Sec. IX, which included two tensile tests on the weldment in accordance with ASTM E8 and four (4) side bending tests using ASTM E190-14.

Table 1. Base metal grouping based on ASME BPVC Sec. IX

Spec. No.	Grade	UNS No.	Minimum specified Tensile (MPa)	P-No.	Group No.	Nominal Composition
A/SA-790	S31803	S31803	620	10H	1	22Cr–5Ni–3Mo–N

Table 2. Base metal chemical composition

Material DSS 31803	C	Mn	Si	Cr	Ni	Mo	N	P	S
Standard values	≤0.030	≤2.00	≤1.00	22.0-23.0	4.5-6.5	3.0-3.5	0.14-0.20	≤0.030	≤0.020
Measured values	0.031	1.508	0.357	22.60	5.988	2.991	0.134	0.012	<0.0003

Table 3. GTAW Electrode chemical composition

Material ER 2209	Mn	C	Cr	Si	Ni	N	Mo	P	S
Measured values	1.75	0.023	22.44	0.57	8.91	0.18	2.85	0.017	0.012

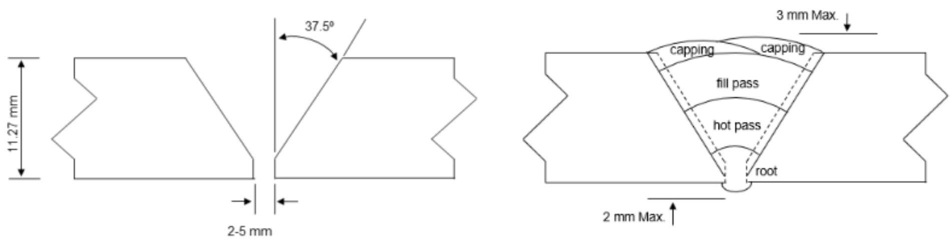

Figure 3. Welding groove and welding sequences

Table 4. Welding parameter

Process	Weld bead	Filler metal	Diameter (mm)	Polarity	Current range (A)	Voltage range (V)	Welding speed (mm/minutes)
GTAW	Root pass	ER2209	2.4	DC EN	80 – 120	9 - 13	50 – 90
GTAW	Hot pass	ER2209	2.4	DC EN	90 – 125	9 - 13	55 - 100
GTAW	Filling pass	ER2209	2.4	DC EN	120 – 160	10 - 14	55 - 100
GTAW	Capping	ER2209	2.4	DC EN	95 -130	10 - 14	55 - 95

3. Result and Discussion

3.1. Macrostructure appearance of weld joint

Figure 4 shows the macrostructure of the etched DSS UNS 31803 pipe weld joint. Morphologically, from bottom to top, it is a sequence of weld layers starting from the root pass, hot pass, filling, and capping. Meanwhile, the heat affected zone (HAZ) area on duplex weldment, cannot be seen on macro-observations, because the boundary between weld metal and base metal is clearly visible, unlike HAZ in carbon steel welded joints.

IOP Conf. Series: Earth and Environmental Science 1151 (2023) 012056 doi:10.1088/1755-1315/1151/1/012056

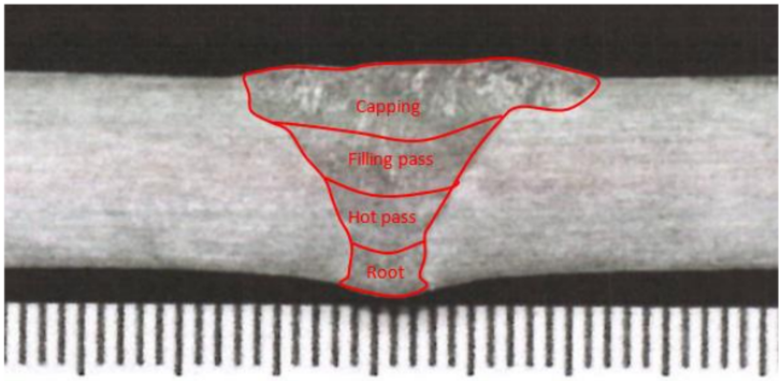

Figure 4. Weld joint macrostructure's morphology consisted of root, hot pass, filling, and capping

3.2. Microstructure Observation and Analysis

There are quite striking differences in the microstructure of the base metal and weld metal. In the base metal, the ferrite (α) structure is observed to resemble a gray ocean, and the austenite (γ) structure is observed as islands with a whiter color and arranged quite regularly, as shown in Figure 5a. The structure of the weld metal represented by the root weld (5b) and capping (5c) shows the presence of a dendritic authenticite (γ-dendritic) phase which is shaped like an irregular long strip and distributed at the ferrite grain boundary. From the statistical calculation of ferrite content using the manual point count method based on ASTM E-562, it was found that the ferrite phase decreased in weld metal, with a value of about 40±2% for root welds and about 45±1% for capping, as also observed by [15].

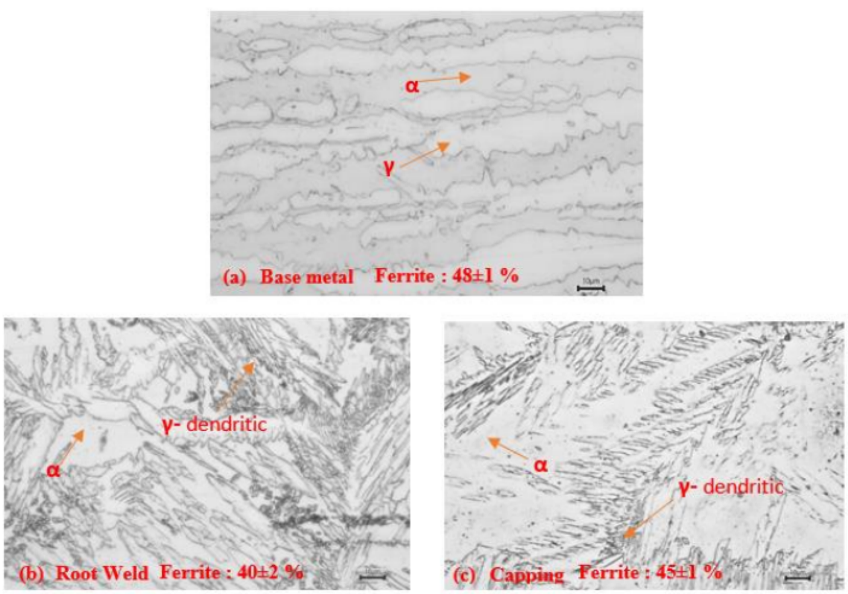

Figure 5. Weld joint microstructure at 500x and their ferrite content at (a) base metal; (b) root; and (c) capping

In the observation of the microstructure with a magnification of 200x, it can be seen that the HAZ, the transition area between the base metal and the weld metal near the root-pass and hot-pass, as shown in Figure 6. In the HAZ area near the root, the dendritic austenite phase (tree-like structure) is dispersed in the form of small blocks in the ferrite grain boundaries, while the area near the hot-pass observed dendritic austenite phase in the form of needles and longitudinal strips. During the duplex welding process, heating occurs at high temperatures in a relatively short time which can cause precipitation, or an intermetallic stage in the form of a sigma phase in both the ferrite and austenite regions. Figure 7 shows the austenite phase precipitation in the form of columnar and dendritic in the ferrite grains that occur in the weld metal.

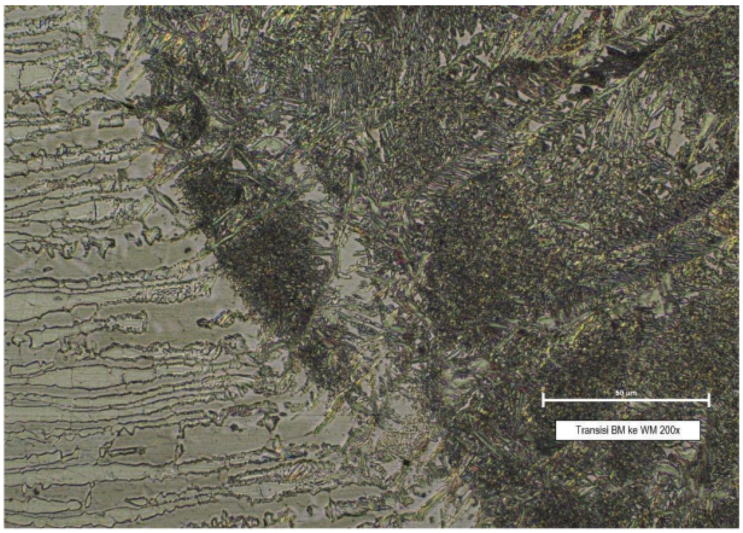

Figure 6. Microstructure of weld joint transition between base metal and HAZ at 200x

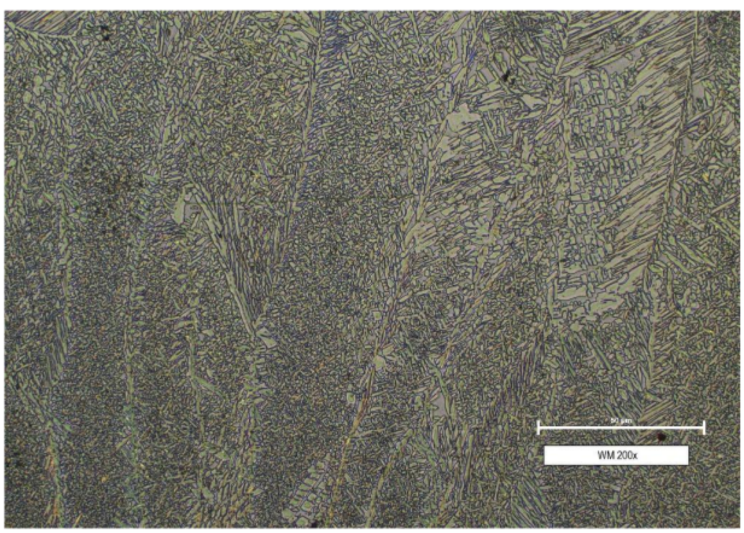

Figure 7. Microstructure of weld metal at 200x

3.3. *Analysis of Mechanical Properties*

According to Table 5, two tensile test specimens that were broken on base metal had welded joint strengths of 844 MPa and 834 MPa, respectively, and were deemed to have experienced ductile failure. The measured tensile strengths are higher than the required 620 MPa value, indicating that the strength of two welded joints complies with the standards. Table 6 shows that the four-side bending specimen test produced no cracks, indicating that the two-welded joint's toughness is good.

Table 5. Tensile test result

Specimen No	Thickness (mm)	Width (mm)	Area (mm2)	Tensile load (N)	Tensile Strength (N/mm2)	Location of failure	Type of failure
TS-1	11.04	19.08	210.643	177716	844	Base metal	Ductile
TS-2	11.36	19.23	218.453	182247	834	Base metal	Ductile

Table 6. Side bend test result

Specimen No.	Observation	Results
Side Bend-1	No open discontinuity was observed	Accepted
Side Bend -2	No open discontinuity was observed	Accepted
Side Bend -3	No open discontinuity was observed	Accepted
Side Bend -4	No open discontinuity was observed	Accepted

3.4. *Pitting Corrosion*

Pitting corrosion test was conducted on a girth weld specimen, in accordance with ASTM G48-11 method A specification. The sample was subjected to 24 hours of total immersion in 600 mL $FeCl_3.6H_2O$ (ferric chloride hexahydrate), at constant temperature of 22 ± 2°C. Observation from the specimen after immersion found that no pitting corrosion on concerned area was observed at 20x magnification with weigh loss 1.7 g/m^2.

4. Conclusion

In the present study, manual GTAW butt welding of A/SA 790 UNS31803 dupex stainless steel was carried out and tested mechanically, physically, and the corrosion behaviour analysed. The main finding is that there is a higher concentration of ferrite in base metal than in weld metal, possibly as a result of secondary phase precipitation. It has also been noted that a large quantity of dendritic austenite phases are distributed along the ferrite grain boundary, whereas a smaller proportion of dendritic austenite phases are distributed elsewhere. Both tensile and bending test result shows that the standard required for the procedure qualification record as stated in ASME BPVC Sec. IX were fulfilled. The pitting corrosion resistance of the weldment shows that the weight loss is about 1.7 g/m^2, which still below the project requirement and no pitting corrosion was observed after immersion test in ferric chloride hexahydrate solution as ruled in ASTM G-48 method A.

Acknowledgements

Authors would like to thank the following institutions who have helped us undertake this research. Firstly, Detech Material Testing Laboratory for facilitating the material testing, and secondly Institut Teknologi Nasional Yogyakarta (ITNY) for funding this publication.

References

[1] Purwanto W W, Muharam Y, Pratama Y W, Hartono D, Soedirman H and Anindhito R 2016 Status and outlook of natural gas industry development in Indonesia *Journal of Natural Gas Science and Engineering* **29** 55–65

[2] Anonim 2022 Welding technology of 2205 duplex stainless steel https://www.epowermetals.com/welding-technology-of-2205-duplex-stainless-steel.html

[3] Hou Y, Nakamori Y, Kadoi K, Inoue H and Baba H 2022 Initiation mechanism of pitting corrosion in weld heat affected zone of duplex stainless steel *Corros. Sci.* **201**

[4] Sakata M, Kadoi K and Inoue H 2021 Acceleration of 475 °C embrittlement in weld metal of 22 mass% Cr-duplex stainless steel *Mater. Today Commun.* **29**
[5] Makhdoom M A, Ahmad A, Kamran M, Abid K and Haider W 2017 Microstructural and electrochemical behavior of 2205 duplex stainless steel weldments *Surfaces and Interfaces* **9** 189–195
[6] Xie X F, Li J, Jiang W, Dong Z, Tu S T, Zhai X and Zhao X 2020 Nonhomogeneous microstructure formation and its role on tensile and fatigue performance of duplex stainless steel 2205 multi-pass weld joints *Materials Science and Engineering: A* **786** 139426
[7] Luo J, Dong Y, Li L and Wang X 2014 Microstructure of 2205 duplex stainless steel joint in submerged arc welding by post weld heat treatment *J. Manuf. Process* **16**(1) 144–148
[8] Han L, Han T, Chen G, Wang B, Sun J and Wang Y 2021 Influence of heat input on microstructure, hardness and pitting corrosion of weld metal in duplex stainless steel welded by keyhole-TIG *Mater. Charact.* **175** 111052
[9] Köse C 2021 Dissimilar Laser Beam Welding of AISI 420 Martensitic Stainless Steel to AISI 2205 Duplex Stainless Steel: Effect of Post-Weld Heat Treatment on Microstructure and Mechanical Properties *J. Mater. Eng. Perform.* **30**(10) 7417–7448
[10] Zheng C, Zhang C, Wang X Y and Gu J 2021 Investigation of mechanical and corrosion behavior of laser hybrid weld joint of 2205 duplex stainless steel *Anti-Corrosion Methods and Materials* **68**(5) 357–364
[11] Bharathi R S, Shanmugam N S, Kannan R M and Vendan S A 2018 Studies on the Parametric Effects of Plasma Arc Welding of 2205 Duplex Stainless Steel *High Temperature Materials and Processes* **37**(3) 219–232
[12] Zhang Y, Liu Z and Li D 2021 Influence of aging temperature on metallurgy, impact toughness and pitting behavior of flux-cored arc welded 2205 duplex stainless steel joint *Mater. Trans.* **62**(6) 756–762
[13] Tóth T, Krasnorutskyi S, Hensel J and Dilger K 2021 Electron beam welding of 2205 duplex stainless steel using pre-placed nickel-based filler material *International Journal of Pressure Vessels and Piping* **191**
[14] Emami S, Saeid T and Abdollah-zadeh A 2019 Effect of friction stir welding parameters on the microstructure and microtexture evolution of SAF 2205 stainless steel *J. Alloys Compd.* **810**
[15] Li L, Du Z, Sheng X, Zhao M, Song L, Han B and Li X 2022 Comparative analysis of GTAW+ SMAW and GTAW welded joints of duplex stainless steel 2205 pipe *International Journal of Pressure Vessels and Piping* **199** 104748
[16] Varbai B, Pickle T and Májlinger K 2019 Effect of heat input and role of nitrogen on the phase evolution of 2205 duplex stainless steel weldment *International Journal of Pressure Vessels and Piping* **176**
[17] IX A S 2015 Qualification standard for welding, brazing, and fusing procedures *ASME Int* **9** 1-24

Investigation of mechanical, microstructure, and corrosion properties of duplex stainless steel joint for natural gas processing facilities

ORIGINALITY REPORT

18%	11%	14%	8%
SIMILARITY INDEX	INTERNET SOURCES	PUBLICATIONS	STUDENT PAPERS

PRIMARY SOURCES

1	Liying Li, Zhaoxia Du, Sheng Xuezhen, Meng Zhao, Lixin Song, Bin Han, Li Xueda. "Comparative analysis of GTAW+SMAW and GTAW welded joints of duplex stainless steel 2205 pipe", International Journal of Pressure Vessels and Piping, 2022 Publication	2%
2	Saeid Mokhatab, William A. Poe, John Y. Mak. "Basic Concepts of Natural Gas Processing", Elsevier BV, 2019 Publication	2%
3	backend.orbit.dtu.dk Internet Source	2%
4	coek.info Internet Source	2%
5	St Sabahannur, Suraedah Alimuddin, St Subaedah, Nurul Wahdaniya, Firda Yunita Faharuddin. "The Effect of Cocoa Butter Substitute (CBS) Produced from Palm Kernel	2%

Oil and Virgin Coconut Oil (VCO) on The Quality of Milk Chocolate", Research Square Platform LLC, 2023
Publication

6	ebin.pub Internet Source	1 %
7	A Y Chaudhari, D D Deshmukh. "Metallurgical investigations on corrosion behavior of simple and heat treated duplex stainless steel 2205 exposed to corrosive media", IOP Conference Series: Materials Science and Engineering, 2020 Publication	1 %
8	iopscience.iop.org Internet Source	1 %
9	pertambangan.fst.uinjkt.ac.id Internet Source	1 %
10	Submitted to Rutgers University, New Brunswick Student Paper	1 %
11	www.mdpi.com Internet Source	1 %
12	Submitted to Universitas Islam Indonesia Student Paper	1 %
13	Ehsan Rahimi, Ali Kosari, Saman Hosseinpour, Ali Davoodi, Henny Zandbergen, Johannes	1 %

M.C. Mol. "Characterization of the passive layer on ferrite and austenite phases of super duplex stainless steel", Applied Surface Science, 2019
Publication

14	Submitted to Universitas Muhammadiyah Yogyakarta Student Paper	1 %
15	www.sciencegate.app Internet Source	1 %
16	R. Neissi, M. Shamanian, M. Hajihashemi. "The Effect of Constant and Pulsed Current Gas Tungsten Arc Welding on Joint Properties of 2205 Duplex Stainless Steel to 316L Austenitic Stainless Steel", Journal of Materials Engineering and Performance, 2016 Publication	1 %
17	mafiadoc.com Internet Source	1 %

Exclude quotes	Off	Exclude matches	< 1%
Exclude bibliography	On		